

# INTERNATIONAL JOURNAL OF CHEMICAL REACTOR ENGINEERING

---

*Volume 4*

2006

*Article A19*

---

## **Design of a Fuel Cell Power System for Automotive Applications**

Panini K. Kolavennu\*

John C. Telotte†

Srinivas Palanki‡

\*Florida State University, panini@eng.fsu.edu

†Florida State University, telotte@eng.fsu.edu

‡Florida State University, palanki@eng.fsu.edu

# Design of a Fuel Cell Power System for Automotive Applications

Panini K. Kolavennu, John C. Telotte, and Srinivas Palanki

## **Abstract**

In this paper, the primary components of a PEM fuel cell for automotive applications, using methane as a fuel, are analyzed. Basic chemical engineering principles are utilized to assess the role of thermodynamics, heat transport, and reaction kinetics. The amount of methane required is calculated as function of hydrogen produced as well as the power produced. The heat duty for thermal control of the system is analyzed.

**KEYWORDS:** fuel cell modeling, hydrogen generation, power system

## 1 INTRODUCTION

Fuel cell power systems for automotive applications have received increased attention in recent years because of their potential for high fuel efficiency and lower emissions [Zalc and Loffler, 2002]. In particular, a fuel cell converts hydrogen and oxygen into water, directly generating electrical energy from chemical energy without being restricted by efficiency limits of the Carnot thermal cycle [Larminie and Dicks, 2000]. This interest in automotive applications has primarily been the result of the breakthroughs made in polymer electrolyte membrane (PEM) fuel cells which have several attractive features such as low operating temperatures (around 350 K), relatively low cost, simple maintenance requirements, and high efficiency.

While there have been significant advances in fuel cell technology, one reason this technology has not seen wide-spread applications in the automotive industry has been the lack of an efficient hydrogen distribution center [Lovins and Williams, 1999] and the difficulties associated with storing hydrogen onboard an automobile [Lovins and Williams, 1999]. One option to alleviate these problems is to develop a system that utilizes a commonly available carbon-based hydrogenous fuel such as gasoline or methane to generate the necessary hydrogen *in situ* on an “as needed” basis. Hydrocarbon fuels are relatively easy to store onboard a vehicle and a nationwide infrastructure to supply these fuels already exists [Dicks, 1996].

In this paper, the primary components of a fuel cell power system, that utilizes methane to generate hydrogen, are analyzed. In particular, basic chemical engineering principles are utilized to design a reactor train that converts methane to hydrogen of the desired purity. The relation between the amount of hydrogen produced and the corresponding amount of methane required is calculated. This relation is utilized in a model of a PEM fuel cell system and the amount of power produced is calculated as a function of hydrogen entering the fuel cell. Finally, the heat duty for thermal control of the reactor train is analyzed. This overall system has many similarities to standard chemical process plants.

However, there are several interesting operational constraints (e.g. reactor size, reactor temperature and pressure) that make the design and operation of this system challenging.

## 2 SYSTEM DESCRIPTION

A schematic of the fuel cell system under consideration is shown in Figure 1. The two main components of the overall system are (1) the fuel processing subsystem and (2) the power generation subsystem. Methane enters the fuel processing subsystem and is converted to hydrogen. Hydrogen enters the fuel cell where it mixes with oxygen to generate electrical power which drives an electric motor. A brief description of the two main subsystems is given below:

### Fuel Processing Subsystem

The fuel processing subsystem consists of three packed bed reactors:

- The steam reformer: In this reactor, methane is converted to hydrogen and carbon monoxide. Part of the carbon monoxide reacts with water to produce carbon dioxide and hydrogen, and

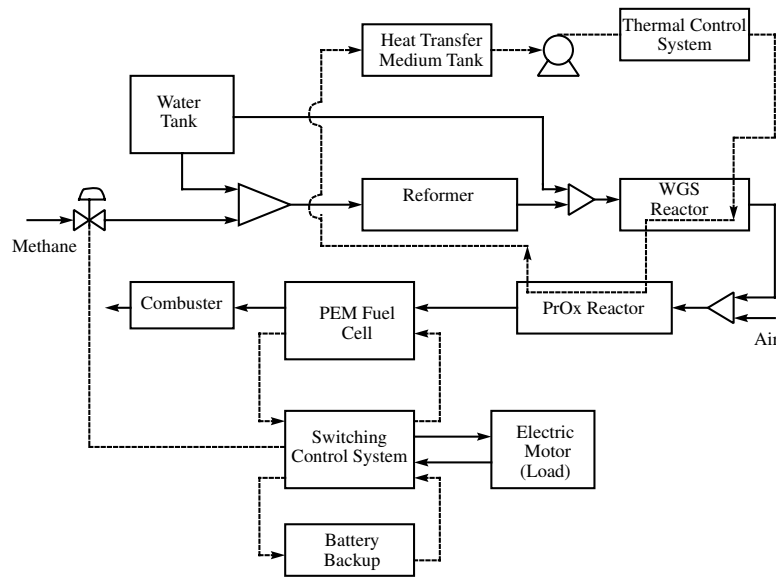
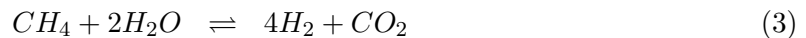
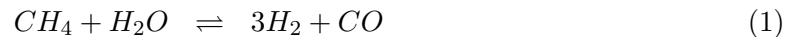


Figure 1: Schematic of Fuel Cell System

some methane is totally oxidized to carbon dioxide. The following reactions occur:



- The water gas shift reactor: In this reactor, most of the remaining carbon monoxide is converted to hydrogen. The following exothermic reaction occurs:



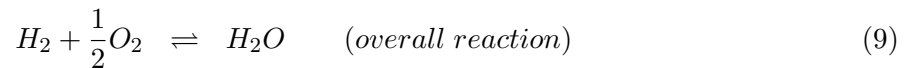
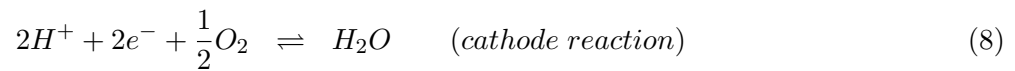
- The preferential oxidation reactor: The water gas shift reaction is limited by equilibrium considerations to a conversion of approximately 80%. Thus, the stream exiting the water gas shift reactor may still have significant amounts of carbon monoxide that can poison the PEM fuel cell electrocatalyst. For this reason, it is necessary to have a preferential oxidation reactor where the carbon monoxide from the water gas shift reactor is reacted with air to form carbon dioxide. Some of the hydrogen reacts with the oxygen to produce water.



The fuel generation subsystem consists of a combination of exothermic and endothermic reactions. The steam reforming reaction is endothermic while the water gas shift reactions and the preferential oxidation reactions are exothermic. Thus, proper thermal management is required to efficiently utilize the heat generated by the exothermic reactions in the reactors where heat is required.

## Power Generation Subsystem

The power generation system consists of a PEM fuel cell that utilizes the hydrogen coming from the fuel processing subsystem and converts it into electricity that is used to power an electric motor for the automobile. The following reactions occur in the fuel cell:



The hydrogen comes in at the anode where it splits into hydrogen ions and electrons in the presence of a catalyst. The hydrogen ions pass through the electrolyte towards the cathode. The electrons cannot pass through the electrolyte and so they pass through an external circuit from the anode to the cathode thereby producing a current. At the cathode, the oxygen combines with the electrons and hydrogen ions in the presence of a catalyst to form water.

In addition to the fuel cell, there is a battery backup that the electric motor switches to when the hydrogen delivered to the fuel cell is insufficient to meet the *instantaneous* power demands of the electric motor. This battery backup is essential because significant load transitions occur frequently as a result of sudden acceleration on highway ramps as well as terrain changes [Zalc and Loffler, 2002].

## 3 DESIGN OF FUEL PROCESSING SUBSYSTEM

In this section, we consider the design and operation of a fuel cell system for a rating of 50 kW. This figure may seem low (50 kW = 67 hp) when compared to power ratings of today's internal combustion engines; yet because electric motors deliver maximum torque at all rpms while internal combustion engines deliver maximum torque only at an optimal rpm. Thus internal combustion engines operate at a fraction of their nominal power rating while electric motors operate at their rated power at all times [Zalc and Loffler, 2002].

As described in the previous section, the fuel processor subsystem consists of a train of three tubular reactors. Each reactor is modeled as an isothermal plug-flow reactor. It is assumed that no axial mixing or axial heat transfer occurs. The automotive application puts a constraint on the total volume of the reactor train since the entire system has to fit under the hood of the automobile.

### Steam Reformer

Xu and Froment [1980] developed intrinsic rate expressions for the steam reforming of methane, accompanied by the water gas shift reaction on a  $Ni/MgAl_2O_3$  catalyst. The following reaction

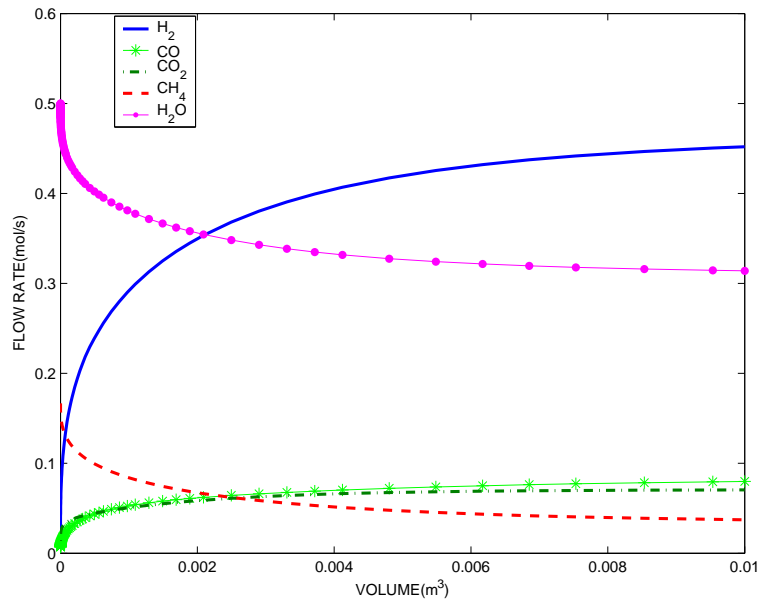


Figure 2: Concentration Profile in Reformer

rate laws were derived:

$$r_1 = \frac{\frac{k_1}{P_{H_2}^{2.5}} \left( P_{CH_4} P_{H_2O} - \frac{P_{H_2}^3 P_{CO}}{K_1} \right)}{\left( 1 + K_{CO} P_{CO} + K_{H_2} P_{H_2} + K_{CH_4} P_{CH_4} + K_{H_2O} P_{H_2O} / P_{H_2} \right)^2} \quad (10)$$

$$r_2 = \frac{\frac{k_2}{P_{H_2}} \left( P_{CO} P_{H_2O} - \frac{P_{H_2} P_{CO_2}}{K_2} \right)}{\left( 1 + K_{CO} P_{CO} + K_{H_2} P_{H_2} + K_{CH_4} P_{CH_4} + K_{H_2O} P_{H_2O} / P_{H_2} \right)^2} \quad (11)$$

$$r_3 = \frac{\frac{k_3}{P_{H_2}^{3.5}} \left( P_{CH_4} P_{H_2O}^2 - \frac{P_{H_2}^4 P_{CO_2}}{K_3} \right)}{\left( 1 + K_{CO} P_{CO} + K_{H_2} P_{H_2} + K_{CH_4} P_{CH_4} + K_{H_2O} P_{H_2O} / P_{H_2} \right)^2} \quad (12)$$

where  $r_1$ ,  $r_2$  and  $r_3$  are the reaction rates for the reactions represented by eq. (1), (2) and (3) respectively. The  $P_i$  are the partial pressures of the reactants and the values of the constants are given in the Appendix.

The steam reformer was simulated as an isothermal packed bed reactor operating at 1000 K and 5.05 bar. The density of the catalyst was assumed to be 210 kg/m<sup>3</sup> and the bed porosity was assumed to be 0.4. The feed to the reactor consisted of steam and methane. The steam to methane ratio was kept at the ratio 3:1 to minimize coking [Dicks, 1996]. The flow rate of methane was set at 0.167 mol/s. Based on these conditions, the reformer volume was found to be 0.01 m<sup>3</sup> for 90% conversion of methane. The amount of hydrogen produced from the reformer was 0.452 mol/s. The concentration profiles along the reactor length are shown in Figure 2.

Temperature (K)	Total Volume ( $m^3$ )
440	0.102
450	0.079
460	0.064
470	0.052
480	0.045
490	0.042
500	0.051

Table 1: Effect of temperature on total volume for 90% conversion

## Water Gas Shift Reactor Design

Choi and Stenger [2003] proposed a kinetic model for the water gas shift reaction on a  $Cu/ZnO/Al_2O_3$  catalyst operating between 400 K to 700 K. The following rate law was developed.

$$r_4 = k_4 P_{CO} P_{H_2O} \left( 1 - \frac{P_{CO_2} P_{H_2}}{P_{CO} P_{H_2O} K_4} \right) \quad (13)$$

where  $r_4$  is the reaction rate for the reaction represented by eq. (4). Other constant values used are given in the Appendix.

This reactor was modeled as a packed bed plug flow reactor. The density of the catalyst was assumed to be  $2355.2 \text{ kg}/m^3$  and the bed porosity was assumed to be 0.4. The feed to the reactor was the stream exiting the reformer. The design of this reactor must be accomplished with the constraint typical of all exothermic reactors. At higher temperatures, the initial reaction rate is very fast; however the equilibrium conversion is low. Conversely, at low temperature, the reaction rate is slow but the equilibrium conversion is high. Figures 3 and 4 show the effect of temperature on the equilibrium conversion possible. To reduce the total volume necessary to achieve at least 90% conversion of carbon monoxide, the water gas shift reactor is split into two zones: a high temperature zone where the reaction rate is high and a low temperature zone where the conversion is high. Simulations at 700 K indicate that an equilibrium conversion of 67% is achieved in a reactor of volume of  $0.001 \text{ m}^3$ . This is modeled as the high temperature zone of the water gas shift reactor. The effect of changing temperature in the low temperature zone on the total volume to achieve an overall conversion of 90% is shown in Table 1. It is observed that operating the low temperature zone at 490 K results in the significant reduction in the total volume. While it is possible to reduce the total volume further by utilizing a continuously decreasing temperature profile, this optimal temperature profile calculation was not attempted given the operational difficulties in experimentally implementing such a temperature profile.

## Preferential Oxidation Reactor Design

The output of the water gas shift reactor still has a considerable amount of carbon monoxide which needs to be reduced to a value below 100 ppm to avoid poisoning the PEM fuel cell membrane [Godat and Marechal, 2003]. The water gas shift reactor outlet stream is mixed with air and fed to a preferential oxidation reactor. This reactor was modeled as an isothermal packed bed reactor.

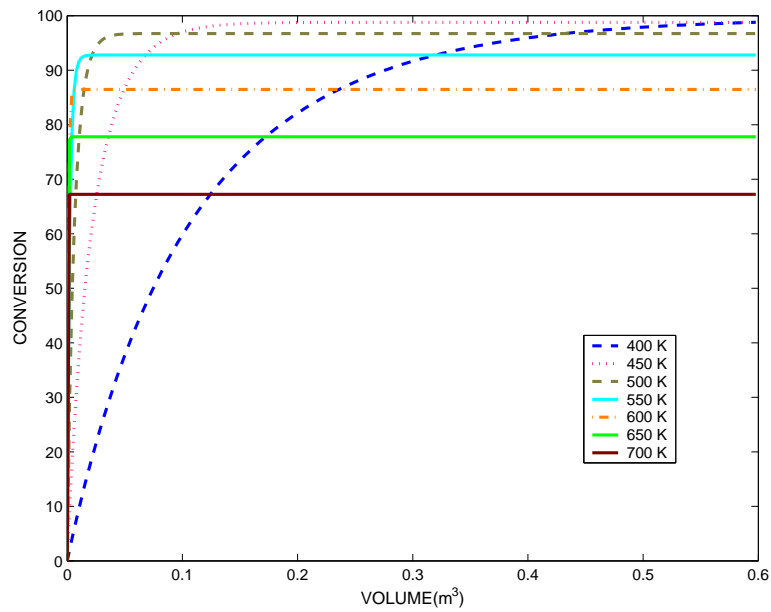


Figure 3: Effect of Temperature in the WGS Reactor

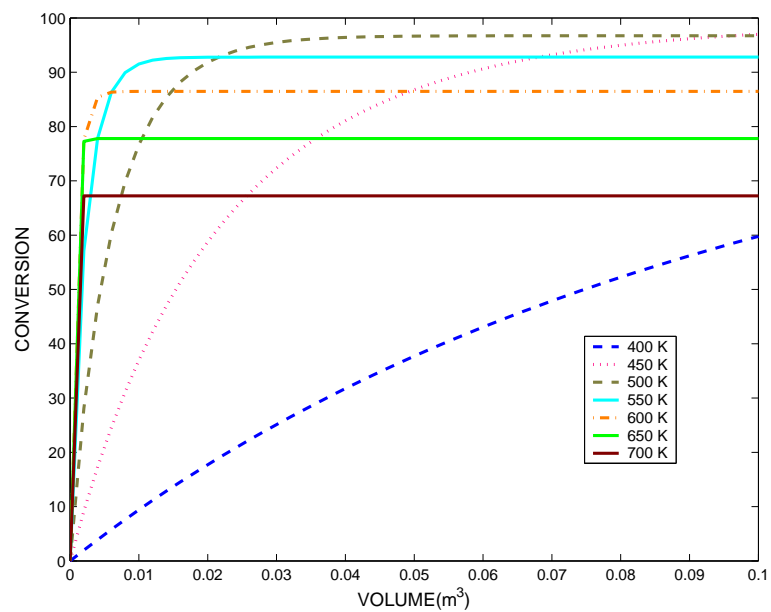


Figure 4: Effect of Temperature in the Initial Part of the WGS Reactor

The density of the catalyst was assumed to be  $210 \text{ kg/m}^3$  and the bed porosity was assumed to be 0.4. The following kinetic model was taken from Kahlich *et al.* [1997].

$$r_5 = k_5 P_{O_2}^{0.40} \left[ \frac{2P_{O_2}}{P_{CO}} \right]^{0.82} \quad (14)$$

$$r_6 = 1.5k_5 P_{O_2}^{0.40} \left[ \frac{2P_{O_2}}{P_{CO}} \right]^{0.82} \quad (15)$$

where  $r_5$  represents the reaction rate of carbon monoxide in the reaction represented by eq. 5 and  $r_6$  represents the reaction rate of hydrogen in the reaction represented by eq. 6. The value of  $k_5$  as a function of  $T$  is given in the Appendix.

The ratio of oxygen in the air to the carbon monoxide exiting the water gas shift reactor was kept at 2:1. A reactor volume of  $3.5 \times 10^{-4} \text{ m}^3$  was sufficient to reduce the carbon monoxide to the desired level of 100 ppm.

### Varying Feed Rates of Methane

In the previous subsections, the reactor train was designed assuming that the feed rate of methane was  $0.167 \text{ mol/s}$ . In this subsection, the effect of changing the feed rate on the overall hydrogen produced using the same reactor train was studied. The methane feed rate to the reformer was varied between  $0.0163 \text{ mol/s}$  and  $0.167 \text{ mol/s}$ . The corresponding steam flow rate was adjusted so that the steam to methane ratio for all the cases studied was maintained at 3:1. The relation between hydrogen exiting the preferential oxidation reactor and the methane entering the reformer is shown in Figure 5. It is observed that the steady state hydrogen production rate varies linearly with the methane feed and can be represented as

$$\dot{N}_{H_2} = 3.12\dot{N}_{CH_4} \quad (16)$$

by fitting a straight line through the data points in Figure 5. This result is not intuitive, as the residence times in the three reactors vary significantly with flow rate. We believe this result indicates that we were operating close to equilibrium.

## 4 DESIGN OF POWER GENERATION SUBSYSTEM

The current generated by the fuel cell stack is directly proportional to the hydrogen consumption rate. The voltage generated by a cell depends on the current density in the cell, thermodynamic parameters (temperature and partial pressures) and the cell materials and design. For a given cell design and thermodynamic state a detailed calculation of the voltage versus current density can be performed. In this work we have utilized a semi-theoretical model first proposed by Larminie and Dicks [2000] and later parameterized by Pukrushpan [2003]. For a fuel cell operating at 353 K with an anode partial pressure of hydrogen of 3 bar and air fed to the cathode at 5 bar, the following cell polarization curve is obtained:

$$V = 0.6405 + 0.3325e^{-i/1000} - 3.036 * 10^{-6}i - 3.55 * 10^{-15}i^3 \quad (17)$$

This relation is plotted in Figure 6. It should be noted that for these conditions that there is a sharp drop-off in cell voltage at small current densities but a very flat region to the polarization

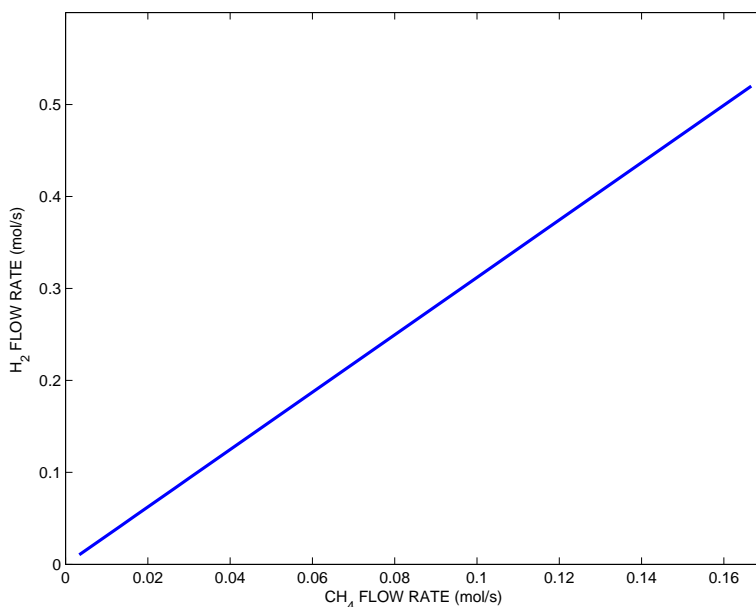


Figure 5: Effect of Flowrate Change on the Hydrogen Production

curve with cell voltages being nearly 0.6 V over a wide range of current densities. This is desirable characteristic as this produces a power density that varies nearly linearly with current density, as seen in Figure 7. This also allows the cells to operate at higher current densities than that found in fuel cells operating near atmospheric pressure.

The design objective for this project has been for a 50 kW fuel cell stack. We have based our design on a cell voltage of 0.6 V. This occurs for a current density of  $1.15 \times 10^4 \text{ A/m}^2$ . If one desires a system with a 300 volt output [Pukrushpan, 2000], then 500 cells in series are required. To generate 50 kW of power then requires 166.67 A of current at 300 volts which requires an active cell area of  $0.0145 \text{ m}^2$ . The required hydrogen flow per cell is calculate from

$$I = 2FX\dot{N}_{H_2} \quad (18)$$

The hydrogen utilization is assumed to be 90%, which yields a maximum required hydrogen flow of  $0.001 \text{ moles/s/cell}$ . This corresponds to a total required methane flow of  $0.153 \text{ mol/s}$ . The power curve for the combined fuel processor and fuel cell stack system is shown in Figure 8. To construct this curve a methane flow rate was selected and the resultant hydrogen flow from the fuel processor was calculated using equation (16). Using equation (18), the cell current was then determined. With the cell area specified at  $0.0145 \text{ m}^2$ , the current density could then be found and the stack power was finally calculated using equation (17) to generate Figure 7. The overall power output versus methane flow into the reformer is shown in Figure 8.

We have also estimated the total stack size based on our design criteria and sizes of commercially available units. If the cell membranes are square the length of the active area will be roughly 0.12 m. We assume 20% increase in this dimension to account for the support frame and gas distribution channels. The Ballard Mark V cell has a depth of 0.38 m for a 35 cell stack which suggests that a 50 cell stack would be roughly 0.54 m in depth. To get 500 cells, one would have ten 50-cell stacks in series. These dimensions can be combined to yield a total stack volume of about  $0.113 \text{ m}^3$ . We

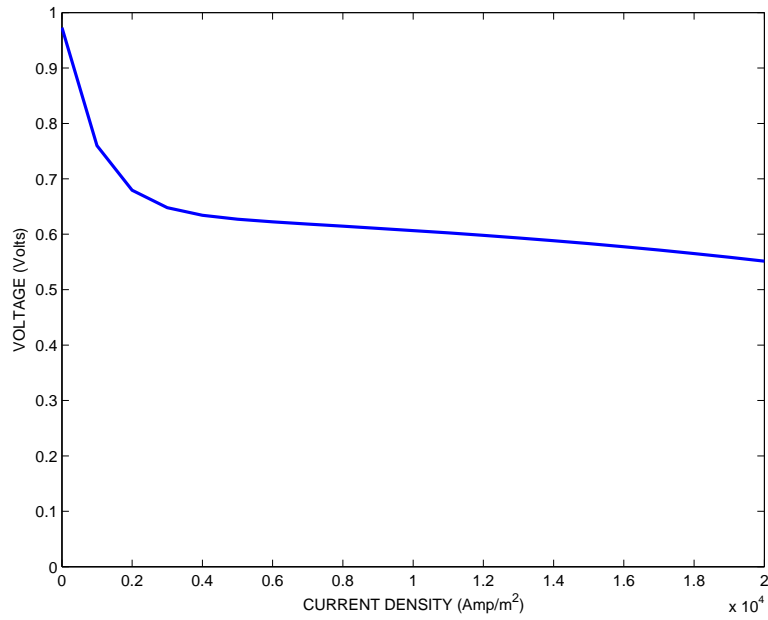


Figure 6: Polarization Curve

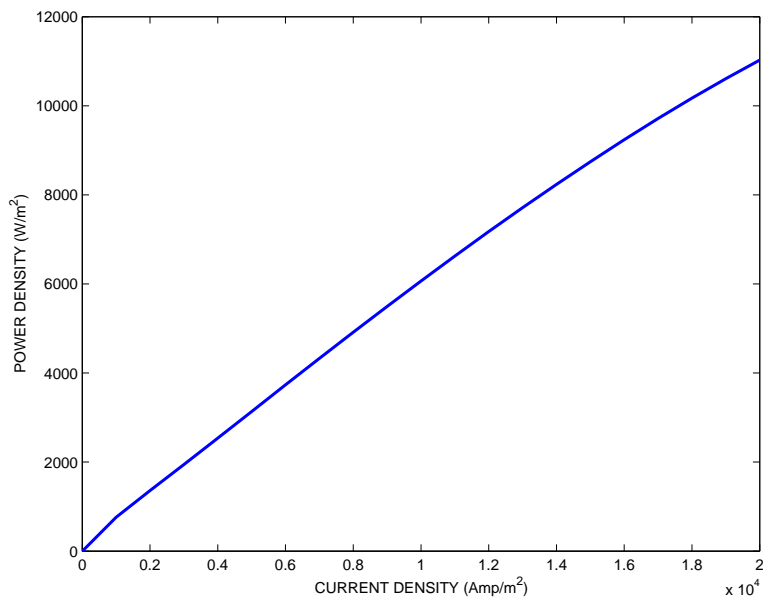


Figure 7: Power density vs. current density

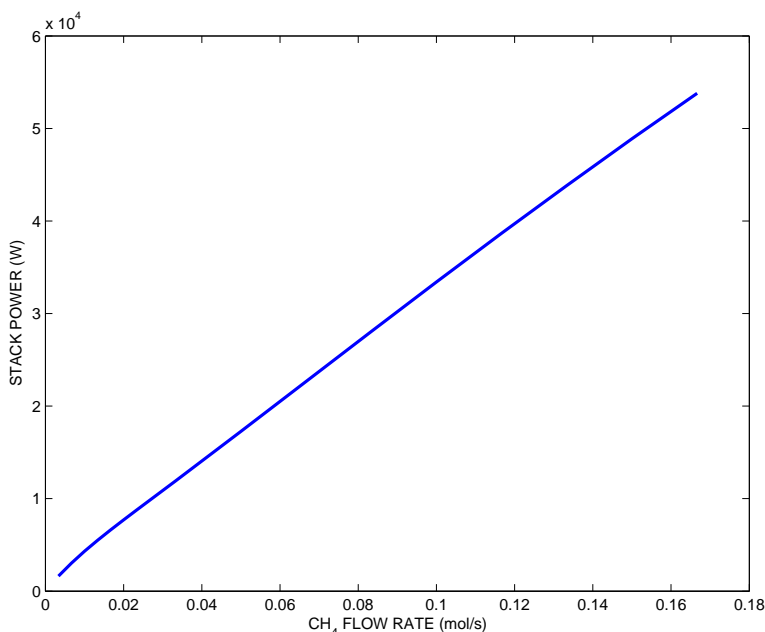


Figure 8: Effect of Methane Flow on Power Generated

added another 20% to the overall system size to account for the ancillary pump for the thermal management system and air compressor plus additional fuel cells to account for inefficiencies. Thus the total system for fuel processing and power generation would occupy roughly  $0.20 \text{ m}^3$  of space.

## 5 ENERGY AND PROCESS INTEGRATION

The system designed above is now analyzed for designing a heat management system. An overall energy balance of the system was conducted at several different flow rates of methane to determine if it is necessary to heat or cool the system. Table 2 shows the difference between the enthalpy of the stream coming out of the preferential oxidation reactor and the stream going into the reformer.

It is observed that it is necessary to provide heat to the fuel processing subsystem. The stream coming out of the fuel cell anode has some unreacted methane and hydrogen. This anode tail gas can be burned in a post-combustion subsystem to generate the necessary heat for the fuel processing subsystem. The heat is to be supplied to the reformer at a 1000 K. Hence, the combustor should operate with at least a 10 K difference in temperature. The lower the operating temperature of the combustor the higher the heat that is liberated from the combustor. The amount of heat liberated by the combustor, if the combustor is operated at 1020 K and assuming complete combustion of the anode tail gases, is given in Table 2. From the table it is clear that this stream does not provide sufficient heat and it may be necessary to feed approximately 33% more methane than that calculated by Figure 5 to account for the heat necessary for the fuel processor subsystem.

This study focuses on the steady state analysis of hydrogen generation from methane. An au-

Methane Flow Rate mol/s	Heat Necessary for Fuel Processing System(kW)	Heat Available from Anode Tail Gas(kW)
0.016	4.57	1.48
0.032	9.13	2.97
0.048	13.30	4.44
0.064	17.65	5.94
0.08	22.77	7.45
0.096	26.64	9.03
0.112	31.03	10.67
0.128	35.41	12.41
0.144	39.57	14.24
0.166	45.43	16.98

Table 2: Heat Duty Calculation

tomobile that utilizes this technology would require a battery backup which would be used for establishing initial reactor temperature as well as for situations where the fuel processor is unable to provide the necessary power instantaneously (e.g. rapid acceleration).

## 6 CONCLUSIONS

The purpose of this paper was to generate an integrated model for the steady-state operation of a PEM fuel cell for automotive operation that utilizes methane as a fuel source. We have utilized kinetic models available in the literature for designing the fuel processing part of this problem. The total volume required for the fuel processor to generate hydrogen of the required purity is about  $0.052 m^3$ . The volume of the power generation system is about  $0.144m^3$ . This equipment can be easily accommodated under the hood of most cars.

This paper demonstrated that it was feasible to use methane as a source of hydrogen. It is possible to utilize higher hydrocarbons such as gasoline and diesel fuel instead of methane as a source of hydrogen since well-developed distribution systems for such fuels are currently available. The design methodology outlined in this paper is valid for higher hydrocarbons as well. The kinetic expressions in the steam reformer will have to be suitably modified to account for additional cracking reactions generated by higher hydrocarbons [Brown, 2001].

Crucial to the effective operation of such a propulsion system is its overall energy efficiency. An overall energy balance indicates that some extra methane might be required to be burned to satisfy the energy requirements of the endothermic reactions. This will be a crucial design feature for real systems and essential to understand for development of the thermal control system [Godat and Marechal, 2003].

## NOMENCLATURE

$A(K)$	pre-exponential factor
$A_c$	area, $m^2$
$E_a$	Activation Energy, $kJ/mol$
$F$	Faraday's constant, 96,485 coulombs/mole
$i$	current density, $Amp/m^2$
$I$	current, $Amps$
$k$	rate constant
$K$	equilibrium constants or adsorption coefficients
$N_c$	number of cells
$\dot{N}_{H_2}$	flow rate of Hydrogen, $mol/s$
$\dot{N}_{CH_4}$	flow rate of Methane, $mol/s$
$P$	power, $kW$
$r$	reaction rate $mol/s/m^3$
$R$	gas constant, $kJ/mol/K$
$V$	voltage, $V$
$X$	hydrogen utilization in the fuel cell

## References

- [1] Brown, L.F., "A comparative study of fuels for on-board hydrogen production for fuel-cell-powered automobiles," *Int. J. Hydrogen Energy*, 26, 381-397 (2001)
- [2] Choi, Y., and Stenger, H.G., "Water gas shift reaction kinetics and reactor modeling for fuel cell grade hydrogen," *J. Power Sources (in press)* (2003)
- [3] Dicks, A.L., "Hydrogen generation from natural gas for the fuel cell systems of tomorrow," *J. Power Sources*, 61, 113-124 (1996)
- [4] Godat, J. and Marechal, F., "Optimization of a fuel cell system using process integration techniques," *J. Power Sources*, 118, 411-423 (2003)
- [5] Kahlich, M.J., Gasteiger, H.A., and Behm, R.J., "Kinetics of selective CO oxidation in  $H_2$  rich gas on  $Pt/Al_2O_3$ ," *J. Catalysis*, 171, 93-105 (1997)
- [6] Larminie, J., and Dicks, A., *Fuel Cell Systems*, Wiley, New York, 2000
- [7] Lovins, A.B., and Williams, B.D., "A strategy for the hydrogen transition," *10th Annual! U.S. Hydrogen Meeting*, Vienna, Virginia, April 1999
- [8] Pukrushpan, J. T., *Modeling and Control of Fuel Cell Systems and Fuel Processors*, PhD thesis, The University of Michigan, Ann Arbor, 2003
- [9] Xu, J.G., and Froment, G.F., "Methane Steam Reforming, Methanation And Water-Gas Shift .1. Intrinsic Kinetics," *AIChE J.*, 35(1), 88-96 (1989)
- [10] Zalc, J.M., and Loffler, D.G., "Fuel processing for PEM fuel cells: transport and kinetic issues of system design," *J. Power Sources*, 111, 58-64 (2002)

## APPENDIX

The rate expressions for the steam reformer are given by equations (10), (11) and (12). The adsorption coefficients can be found using the following relations for the respective species

$$K_i = A(K_i) \exp\left(\frac{-\Delta H_i^o}{RT}\right), \quad \text{where } i = H_2, CO, CH_4, H_2O \quad (19)$$

The rate constants for the three reactors are given by a similar Arrhenius type equation.

$$k_j = A'(k_j) \exp\left(\frac{-E_{a,j}}{RT}\right), \quad \text{where } j = 1, 2, 3, 4, 5 \quad (20)$$

The equilibrium constants for the reactions are given by the following expression,

$$K_j = \exp\left(A_j + \frac{B_j}{T}\right) \quad \text{where } j = 1, 2, 3, 4 \quad (21)$$

The parameters involved are listed in the table below.

Parameter	Value
$A_1$	29.3014
$A_2$	-4.35369
$A_3$	25.225
$A_4$	-4.33
$A'(k_1)$	$1.6369 \cdot 10^{15}$ , [ $mol \cdot bar^{0.5} / (m^3 \cdot s)$ ]
$A'(k_2)$	$7.8780 \cdot 10^5$ , [ $mol \cdot bar^{-1} / (m^3 \cdot s)$ ]
$A'(k_3)$	$3.9506 \cdot 10^{14}$ , [ $mol \cdot bar^{0.5} / (m^3 \cdot s)$ ]
$A(K_{H_2})$	$6.128 \cdot 10^{-9}$ , [ $bar^{-1}$ ]
$A(K_{CO})$	$8.230 \cdot 10^{-5}$ , [ $bar^{-1}$ ]
$A(K_{H_2O})$	$1.77 \cdot 10^5$
$A(K_{CH_4})$	$6.650 \cdot 10^{-4}$ , [ $bar^{-1}$ ]
$B_1$	-26248.4, [ $K^{-1}$ ]
$B_2$	4593.17, [ $K^{-1}$ ]
$B_3$	-21825.28, [ $K^{-1}$ ]
$B_{34}$	4577.8, [ $K^{-1}$ ]
$E_{a,1}$	240.1, [ $kJ / (mol \cdot K)$ ]
$E_{a,2}$	67.13, [ $kJ / (mol \cdot K)$ ]
$E_{a,3}$	243.9, [ $kJ / (mol \cdot K)$ ]
$\Delta H_{H_2}^0$	82.90, [ $kJ / (mol \cdot K)$ ]
$\Delta H_{CO}^0$	70.65, [ $kJ / (mol \cdot K)$ ]
$\Delta H_{H_2O}^0$	-88.68, [ $kJ / (mol \cdot K)$ ]
$\Delta H_{CH_4}^0$	38.28, [ $kJ / (mol \cdot K)$ ]
$A'(k_4)$	$1.005 \cdot 10^7$ , [ $mol \cdot bar^{-2} / (m^3 \cdot s)$ ]
$A'(k_5)$	$3.8629 \cdot 10^9$ , [ $mol \cdot bar^{-0.4} / (m^3 \cdot s)$ ]
$E_{a,WGS}$	47.53, [ $kJ / (mol \cdot K)$ ]
$E_{a,PROX}$	71, [ $kJ / (mol \cdot K)$ ]

Table 3: Kinetic parameters for the three reactors